Polish Journal of Medical Physics and Engineering
The Journal of Polish Society of Medical Physics
ISSN 1898-0309, doi: 10.2478/pjmpe-2023-0013

June 2023
Vol 29, Issue 2

Scientific Paper

# Osseointegration properties of domestic bioactive calcium phosphate ceramics doped with silicon

Vitalii PIDGAIETSKYI[1,ABCDEF,*], Nataliia ULIANCHYCH[2,ABCDEF], Volodymyr KOLOMIIETS[2,ABCDEF], Mykhailo RUBLENKO[3,ABCDEF], Volodymyr ANDRIIETS[3,ABCDEF]

[1]*Department of Traumatology and Orthopaedics of Adults, Institute of Traumatology and Orthopaedics of the National Academy of Medical Sciences of Ukraine, Kyiv, Ukraine*
[2]*Department of Physics of Strength and Plasticity of Materials, Frantsevich Institute for Problems of Materials Science of the National Academy of Sciences of Ukraine, Kyiv, Ukraine*
[3]*Department of Surgery and Small Animal Diseases, Bila Tserkva National Agrarian University, Bila Tserkva, Ukraine*
[*]*Corresponding author: Vitalii Pidgaietskyi; vitali.pidgaietskyi@ukr.net*

(received 13 March 2023; revised 19 May 2023; accepted 30 May 2023)

## Abstract

*Introduction:* The relevance of this study lies in the fact, that today the search for biocompatible materials for the management of bone defects is of importance. Such materials could become an alternative to transplants. For the replacement of bone defects, two-phasic bioactive ceramics of hydroxyapatite and β-tricalcium phosphate is a very attractive biomaterial due to its excellent biocompatibility and osteoconductivity, but the results of its use are quite controversial due to insufficient bioactivity. The purpose of this work is to investigate the osseointegration properties of two-phase bioactive ceramics doped with silicon (HTdSi), both as a single component and a component in combination with platelet-rich fibrin, as well as in comparison with the well-known imported analogue – BIO, which consists of β-tricalcium phosphate, also as an independent component and a component in combination with platelet-rich fibrin. In the experiment, the rabbits of the New Zealand white breed at the age of 3 months and with an average weight of 2.5 kg were used. The terms of implantation are 30, 60, 90 and 180 days. The advantages of the domestic bio-composite are substantiated on the basis of clinical, radiological and histological studies.
*Material and methods:* In the experiment, the rabbits of the New Zealand white breed at the age of 3 months and with an average weight of 2.5 kg were used. The terms of implantation are 30, 60, 90 and 180 days.
*Results:* The osteointegration properties of two-phase bioactive ceramics doped with silicon (HTdSi), both as a single component and in combination with platelet fibrin, were investigated, as well as in comparison with the known imported analog - BIO, which contains β-tricalcium phosphate, both as a single component and in combination with platelet fibrin.
*Conclusions:* The advantages of domestic biocomposite are substantiated on the basis of clinical, radiological and histological studies.

**Keywords**: bioactive calcium-phosphate ceramics; osseointegration; osteoinduction; clinical and radiological studies; histological studies.

## Introduction

Taking into account the rapid development of the possibilities of reconstructive and restorative medicine, which is based on bone tissue regeneration, rather than on its replacement, there is an urgent need for biocompatible materials that would stimulate the formation of bone tissue and could be used in tissue-engineering structures as carriers of living cells.[1-4] The use of autografts and allografts has long been considered the gold standard for bone regeneration in bone defects of various degrees and locations. However, this approach is associated with many complications. In addition to the unavailability and limited amount of autogenous bones, the use of autografts is associated with serious problems such as tissue failure, donor site damage, nerve and vascular damage, chronic pain in the donor site, herniation and surgical risks (bleeding, infection and chronic pain). Allografts do not have these disadvantages, but they integrate more slowly than autografts. They have immunogenicity and can prevent adhesion and differentiation of cells, and their clinical use is relatively limited by complications such as delayed healing and infection, which has led to the search for alternative biomaterials.[4-6]

© 2023 Authors This is an open access article licensed under the Creative Commons Attribution-NonCommercial-NoDerivs License (http://creativecommons.org/licenses/by-nc-nd/4.0/).

Authors' contribution: A – Research concept and design, B – Collection and/or assembly of data, C – Data analysis and interpretation, D – Writing the article, E – Critical revision of the article, F – Final approval of the article.

Due to the analogy with the mineral component of bone tissue, calcium phosphate ceramics (CPC) based on hydroxyapatite (HAP) and β-tricalcium phosphate (β-TCP) is the most common for use in bone tissue plastic from synthetic materials, which have ideal biocompatibility and affinity for bone tissue due to its analogy with the mineral component of bone tissue. However, the possibilities of synthetic osteotropic materials based on calcium phosphates are not fully utilized due to their insufficient bioactivity compared to materials of biological origin. Increasing the bioactivity of CPC and giving it osteoinductive properties is a constant research goal of biomaterials based on calcium phosphates.[7-18] In the publications of recent years, there is more and more information that CPC can have not only good osteoconductive and osteointegration properties but also osteoinductive properties.[1-4,10,13,19,20] The following factors can affect bioactivity: its nanostructuring, polyphasicity, doping with elements that can stimulate cellular activity and creation of compositions with autologous cells.[1,4,10,13,15,21,22] Both increase in solubility and adsorption activity and the activation of interaction with the physiological environment at the cellular level can be the result of the action of these factors.

Therefore, the use of the properties of silicon-containing nanostructured CPC, which affect mesenchymal stem cells, providing genetic control of their vital activity, differentiation and secretory capacity, and imparting osteoinductive properties of CPC by creating combined implants in composition with autocells, can replace materials of biological origin for the restoration of bone tissue. At the same time, nanostructured biomaterials are able to induce osteoblast differentiation in progenitor cells, but despite the progress achieved in CPC production with some surface and solubility properties, the effect of these materials on the organization of cellular processes such as adhesion and differentiation has not yet been sufficiently studied. In particular, questions such as why some biomaterials with CPC can be more osteoinductive than others, and how the material properties contribute to osteoinductivity. The problem of bioactive ceramics in medicine is an interdisciplinary one; therefore, the work approach is to identify the impact of biomaterials on the restoration of bone tissue by specialists in related fields: medical and material science.

In this study, the following issues were evaluated: the microstructure, physicochemical, and biological properties of β-TCP granules and nanostructured porous granules of CPC doped with silicon, both as an independent component and along with platelet-rich fibrin (PRF).

## Materials and Methods

### Characteristics of biomaterials

During the research, the following granules were used:

1. Granules BIO1 BIOSORB (BIO trade name, French production), Dim. 4×4 mm of industrial production, which were crushed to 0.8-1.0 mm. According to the phase composition, according to X-ray phase analysis β-TCP-100%.
2. Granules of two-phase bioactive ceramics doped with silicon, HTdSi (Ukrainian production).

HTdSi was obtained by chemical precipitation from solutions of calcium and phosphate salts ($Ca(NO_3)_2$) and ($(NH_4)_2HPO_4$) with an estimated ratio of Ca/P – 1.6. Silica Asyl-300 (specific surface area 300 $m^2/g$) was used as a silicon source produced by Kalush Test Experimental Plant of ISC (Institute of Surface Chemistry) of the National Academy of Sciences of Ukraine, named after O.O. Chuyka. Silica Asyl-300 was introduced as precipitated, filtered and washed non-stoichiometric HAP in the form of a finely dispersed colloidal solution with mixing in a mixer. The mixture obtained was dried, granulated, and annealed at a temperature of 850°C for one hour. The size of granules ranged from 0.8 to 1.0 mm. Analysis of the chemical composition of HTdSi revealed that the final granules contained 1.2-1.3 wt.%. X-ray phase analysis indicated that the composition consisted of 60% HAP and 40% β-TCP.

The structural composition was controlled by the following methods: X-ray phase analysis (XRF) using an Ultima IV X-ray diffractometer ("Rigaku", Japan) at a wavelength of λ (Cu-Kα-radiation) = 0.154187 nm; The obtained data were processed in the program "PowderCell 2.4", the microscopy of the granules was studied by the method of scanning electron microscopy (SEM). The state of silicon and silver NPs on the surface of the coating with HAP was studied by electron microscopy Tescan Mira (SEM). The microscope was equipped with the HKL CHANNEL 5 system from the OXFORD company – for the diffraction of electrons from a local area with a size of more than 10 nm; the chemical composition was determined using energy dispersive X-ray fluorescence elemental analysis with the use of an express analyzer of chemical composition Expert 3L ("INAM", Ukraine); determination of the adsorption activity of CPC was carried out by saturating the granules with an aqueous solution of methylene blue; the solubility of the materials was determined by the amount of calcium ions concentrations released into a solution that imitates a body fluid; the experimental method consisted in keeping the CPC samples for a day at 37°C in an acetic-acetate buffer solution at pH-5.5 close to the pH of physiological fluid when dissolving of biological hydroxyapatite. Calcium ions in the solution were determined by direct potentiometry using an ion-selective electrode.

### The study of osseointegration properties of biomaterials *in vivo*

Rabbits of the New Zealand white breed at the age of 3 months and with an average weight of 2.5 kg were used in the experiment. All procedures performed using animals were reviewed and approved by the Scientific Ethics Committee of the National Academy of Medical Sciences of Ukraine, Kyiv. Authorization No. 50–32. Rabbits were kept in the vivarium of the university in individual cages in rooms with forced ventilation and combined lighting and daily cleaning in accordance with the sanitary and hygienic requirements of the microclimate parameters and conditions of keeping this species of animals. The feeding consisted of commercially produced compound feed for rabbits according to his instructions. The animals had constant and unlimited access to water. The rabbits were divided into 4 groups of 20 animals each. Imported biocomposite BIO, along with PRF, was used for animals of the first group. Imported biocomposite BIO as an independent component was used for animals of the second group. For the animals of the third group, the defects were filled with granules of biocomposite of HT doped with silicon, which consisted of 80% hydroxyapatite and 20% β-tricalcium phosphate along with platelet-rich fibrin.

The method of obtaining and applying PRF consists of taking blood from a rabbit and immediately centrifuging it for 2-3 minutes, followed by the selection of the liquid part before the polymerization of the fibrin clot and the introduction of this fraction into the defect, which is previously filled with the studied composite material. Granules of biocomposite HT doped with silicon as an independent component were used for the animals of the fourth group to fill defects. Surgery was performed under general anesthesia and analgesia (xylazine – 2 mg/kg in/m, butorphanol – 0.4 mg/kg s/c, sodium thiopental – 6 mg/kg iv, local lidocaine – 3 mg/kg), in compliance with the rules of asepsis and antiseptics. An incision was made from the lateral surface of the distal epiphysis of the femur. At the same time, a bone defect was formed with a drill (d=3 mm). After the completion of the main surgical part, the wounds were sutured with interrupted sutures made of synthetic suture material. On the 30th, 60th, 90th, and 180th days of the experiment, a clinical examination and radiological, macromorphological, and histological studies were conducted. Animals were taken out of the experiment by intravenous injection of thiopental at a dose of 50 mg/kg.

## Results

### Microstructure and physical and chemical properties of biomaterials

Microphotographs (**Figure 1**-**3**) show the surface of granules of HTdSi (A) and BIO (B) at different magnifications: **Figure 1** – magnification 12600, **Figure 2** – magnification 37900, and **Figure 3** – 94800, respectively. Photomicrographs at different magnifications clearly demonstrate the difference in structures of biomaterials. It can be seen in **Figure 1** that HTdSi has a macroporosity significantly greater than BIO, which facilitates rapid integration with bone tissue.

It can be seen in **Figure 2** that BIOs have more mesopores, which contribute to the solubility of the biomaterial.

From the photomicrograph in **Figure 3**, it can be concluded that HTdSi granules have a finer structure with micro- and nano-sized pores, which may indicate the presence of osteoinductive properties.

Studies of the physical and chemical properties of the granules (**Table 1**) confirm this. The presence of a large number of micro and nanopores led to a significant increase in the adsorption activity of HTdSi – more than 10 times. The solubility of biomaterials is almost the same, slightly higher in HTdSi, despite a large number of mesopores in BIO and the greater solubility of β-TCP.

**Table 1. Physico-chemical properties of biomaterials**

| Biomaterial | Phase composition, % | Solubility by ions Ca. g/l | Adsorption activity, mg/g |
|---|---|---|---|
| HTdSi | 40% β-TCP; 60 % HAP | 0.13 | 229.1 |
| BIO | 100% β-TCP | 0.9 | 25.5 |

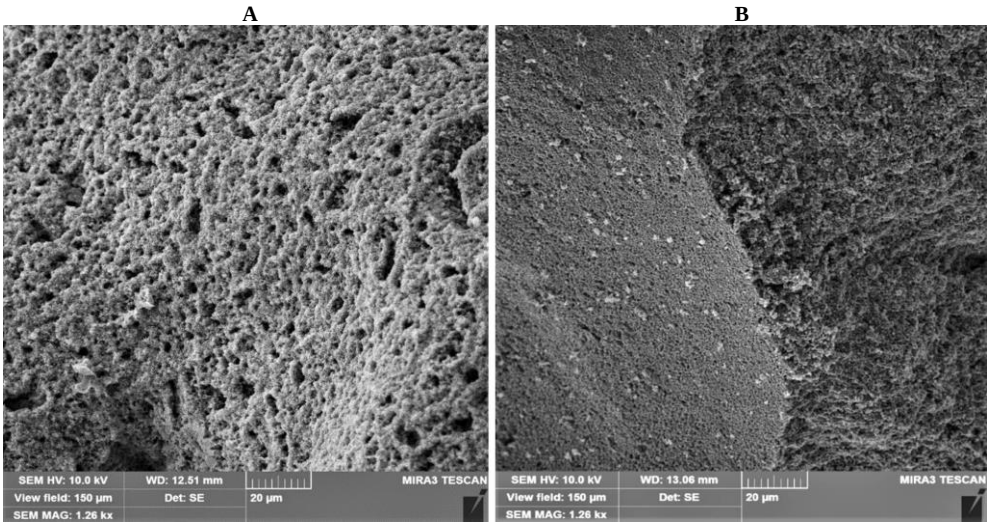



**Figure 1. Microstructure of samples, view field – 150.00 µm (A – HTdSi; B – BIO)**

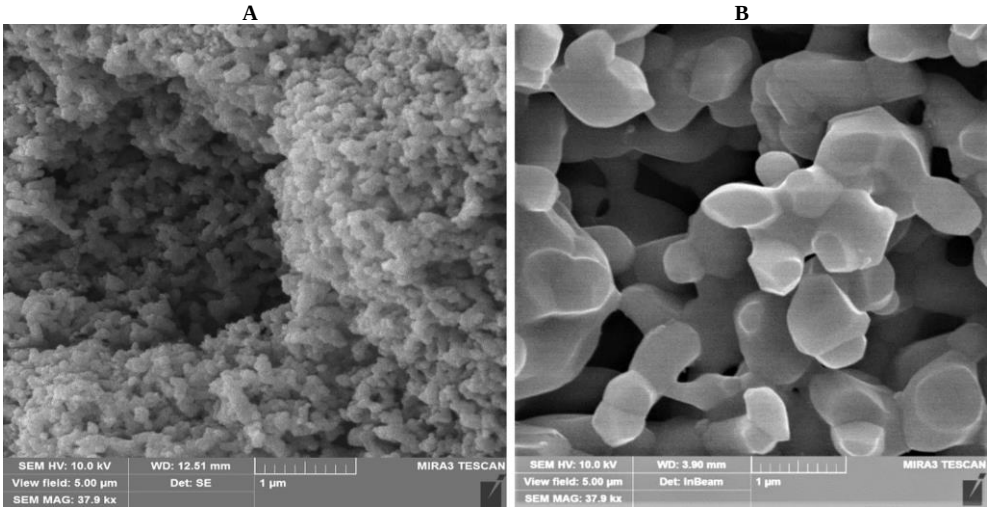



**Figure 2. Microstructure of samples, view field – 5.00 µm (A – HTdSi; B – BIO)**

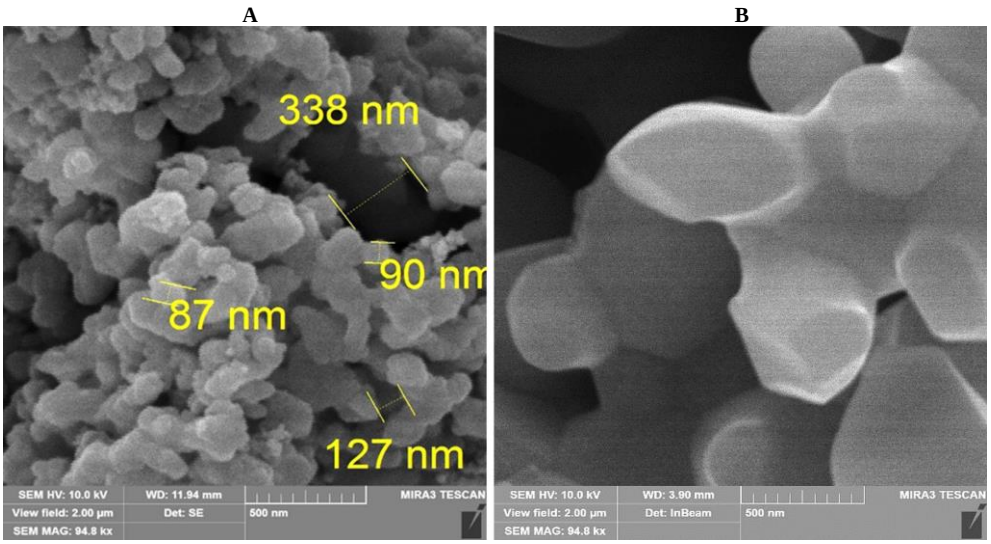



**Figure 3. Microstructure of samples, view field – 2.00 µm (A – HTdSi; B – BIO)**

## Histological and X-ray studies of the defect zone filled with BIO and HTdSi

On the 30th day after implantation of the BIO composite along with PRF (1st group), the presence of the composite was radiologically noted, which was visualized as an area of increased radiodensity that filled the entire defect. On macro-preparation, the implantation site was covered with the newly formed tissue. Histologically, accumulation of stem and semistem osteogenic cells, osteoblasts, collagen fibers, and blood vessels was detected, which indicated the first stage of reparative bone regeneration or the stage of development of osteogenic cells. On the surface of ceramic granules, the initial phase of the second stage of reparative regeneration was noted, which was characterized by the layering of osteoblasts and oxyphilic intercellular substance (organic matrix of bone tissue or osteoid) in these places (**Figure 4**).

On the 30th day after implantation of the BIO composite without PRF (2nd group), the presence of the composite was also noted radiologically, which was visualized as an area of increased X-ray density that completely filled the defect. Composite granules surrounded by the newly formed tissue at the implantation site were visualized on macro-preparation (**Figure 2B**). Histologically, clusters of stem and semi-stem osteogenic cells, osteoblasts, collagen fibers, blood vessels, and individual osteoid islands were detected in the cavities between the granules, which indicated the initial stage of the second stage of reparative bone regeneration. Strips of bone substance (coarse-fibrous bone tissue or primary cancellous bone) formed on the surface of ceramic granules. In some areas, the formation of lamellar bone tissue (secondary cancellous bone) was observed – the transitional stage from the third to the fourth stage of reparative regeneration (**Figure 5**).

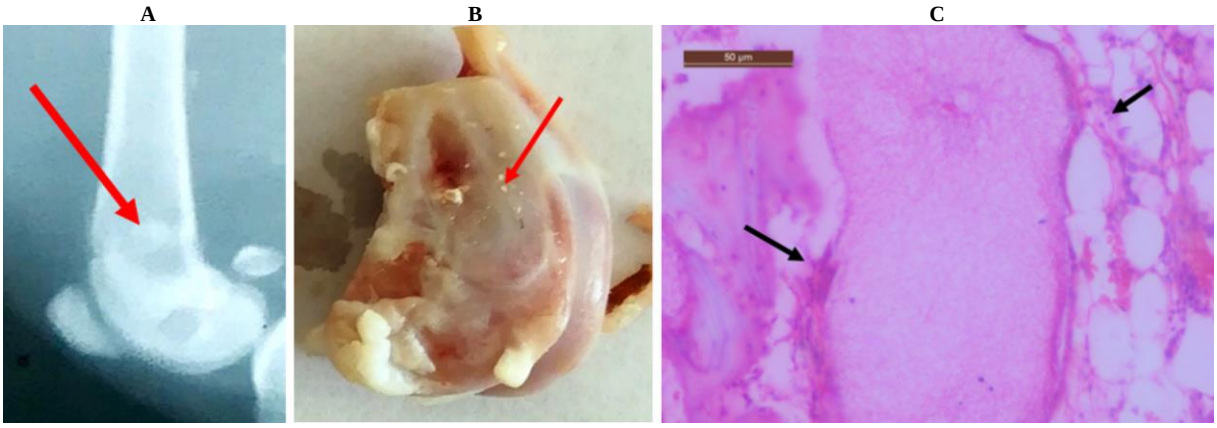



**Figure 4. Day 30. Characteristics of the integration processes of BIO + PRF implants (A – x-ray; B – macroscopic; C – histological)**

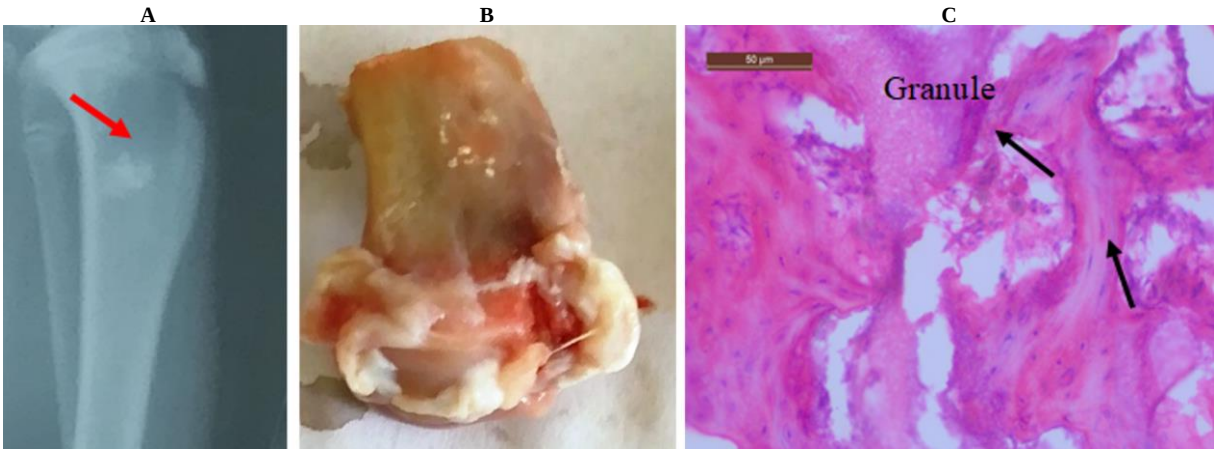



**Figure 5. Day 30. Characteristics of the integration processes of BIO implants (A – radiological; B – macroscopic; C – histological)**

A similar pattern was observed in the 3rd group of animals, where domestic HTdSi bioceramics along with PRF (3rd group) were used. Thus, the presence of a composite was noted radiologically, which was also visualized in the form of an area of increased X-ray density that filled the entire defect. On macro-preparation, the implantation site was covered with the newly formed tissue. The histological picture was similar but with signs of deeper regeneration processes (**Figure 3B**). It was noted here that the structure of ceramic composite granules is in the form of an eosinophilic, fine-grained, homogeneous mass, without signs of destruction, in the form of round-oval conglomerates or congregates. The cavities between ceramic granules are filled with a cluster of stem and semi-stem osteogenic cells, osteoblasts, collagen fibers, and blood vessels. In some areas, osteoid islands (the initial stage of the second stage of reparative bone regeneration) were already present. Strips of bone substance (coarse-fibrous bone tissue or primary cancellous bone) are formed on the surface of ceramic granules. In some areas, the formation of lamellar bone tissue (secondary cancellous bone) is observed, the transition stage from the third to the fourth stage of reparative regeneration (from immature reticulofibrous to mature bone tissue) (**Figure 6**).

In the 4th group of animals, where the domestic HTdSi bioceramics were used to fill the defect as an independent component, the radiograph showed a composite in the form of an area of increased radiological density that filled the entire volume of the defect, as in the previous groups. On macro-preparation, the implantation site was covered by newly formed bone, in which composite granules were visualized. Histologically, it was found that bioceramic granules are an eosinophilic, fine-grained, homogeneous areactive mass, without signs of destruction, in the form of round-oval conglomerates. The cavities between them are filled with a cluster of stem and semi-stem osteogenic cells, osteoblasts, collagen fibers and blood vessels, which is a sign of the first stage of reparative bone regeneration or the stage of development of osteogenic cells. Layering of osteoblasts and an oxyphilic intercellular substance (osteoid) was noted on the surface of ceramic granules. In some areas, the formation of course-fibrous bone tissue is observed: the transitional stage from the second to the third stage of reparative regeneration (transition from osteoid bone to immature coarse-fibrous bone) (**Figure 7**).

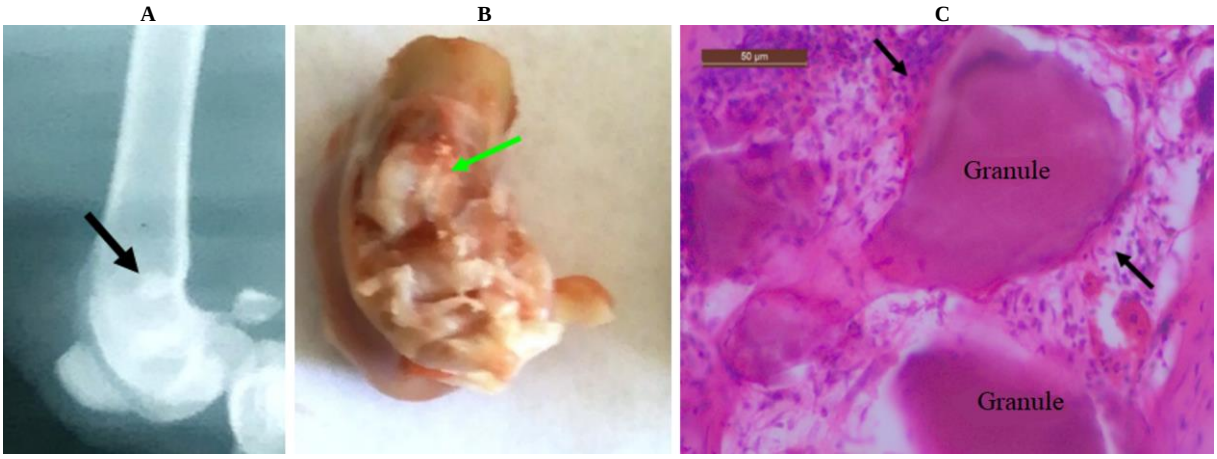



**Figure 6. Day 30. Characteristics of the integration processes of HTdSi + PRF implants (A – radiological; B – macroscopic; C – histological)**

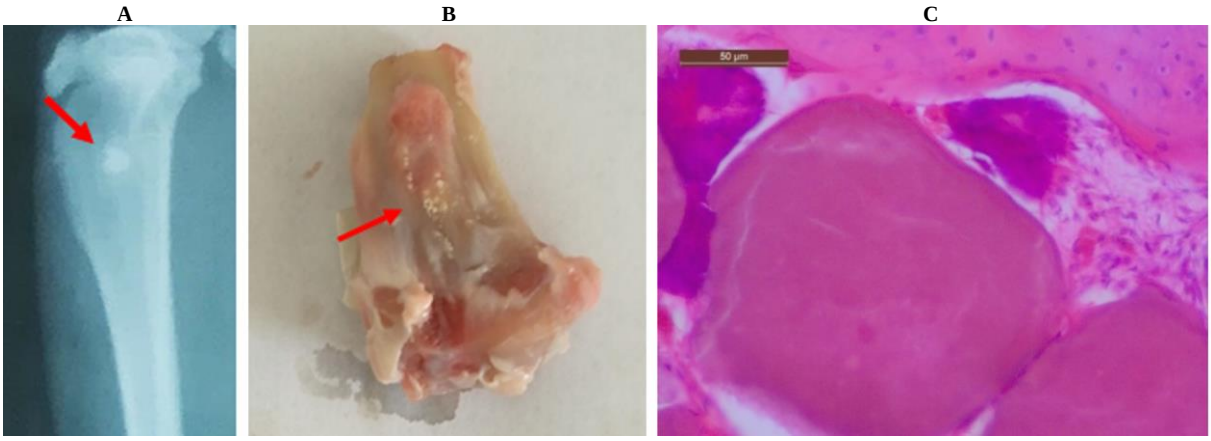



**Figure 7. Day 30. Characteristics of the integration processes of HTdSi implants (A – X-ray; B – macroscopic; C – histological)**

On the 60th day, the appearance between the groups already differed. In particular, in the 1st group of animals, the BIO composite was no longer visualized on radiographs, which indicates the active processes of its resorption. On macros-preparation, the implantation site was covered with bone in the form of periosteal bone growths with significant masses of hyaline cartilage, which covered the entire newly formed bone in the defect area. Histologically, the granules of the composite material had the appearance of a fine-grained eosinophilic homogeneous mass with signs of minor fragmentation and destruction. Between the ceramic granules and on their surface, strips (beams) of course-fibrous bone tissue were found, forming separate cells filled with fibrous connective tissue (collagen fibers, fibroblasts, osteogenic cells, blood vessels). In some areas, osteoid structures were preserved, which indicates the third incomplete stage of reparative regeneration (**Figure 8**).

On the 60th day, in the 2nd animal group, the BIO composite had a non-uniform X-ray density, especially on the periphery of the defect, which indicates the beginning of its resorption in these areas. On macro-preparation, the implantation site was covered with bone in the form of periosteal bone growths with a slight covering of hyaline cartilage in the area of the defect. During the histological examination, the loss of granularity with the acquisition of reticulated fine- and medium-pore structures was noted. Strips (beams) of course-fibrous bone tissue that form individual pores, as in the previous group, but in individual beams, the formation of lamellar bone tissue is observed – the transitional stage from the third to the fourth stage of reparative bone regeneration (from immature reticulofibrous to mature lamellar). Directly on the surface of the ceramic granules, newly formed strips of mainly lamellar bone substance with separate areas of course-fibrous bone tissue are the unfinished fourth stage of reparative bone regeneration (**Figure 9**).

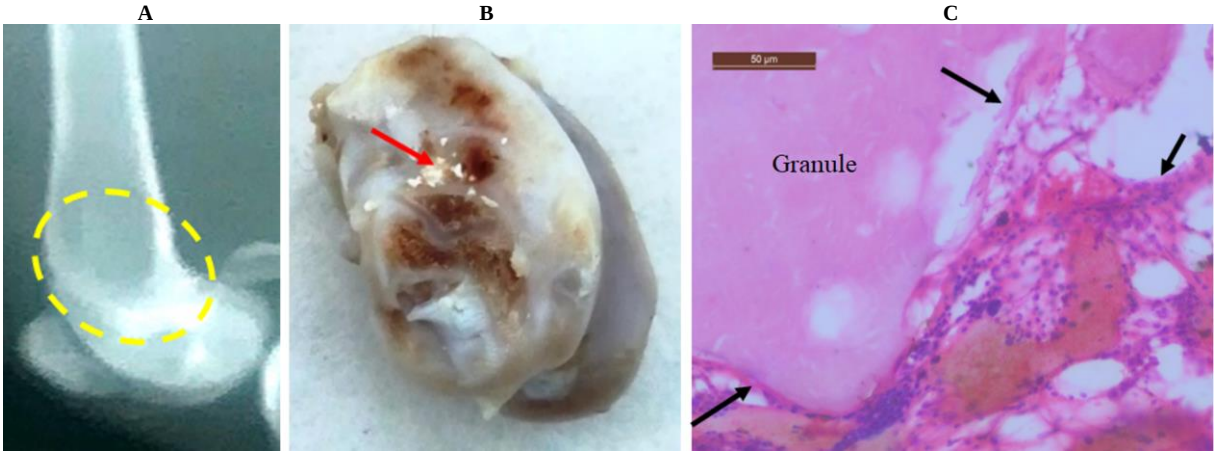



**Figure 8. Day 60. Characteristics of the integration processes of BIO+PRF implants (A – X-ray; B – macroscopic; C – histological)**

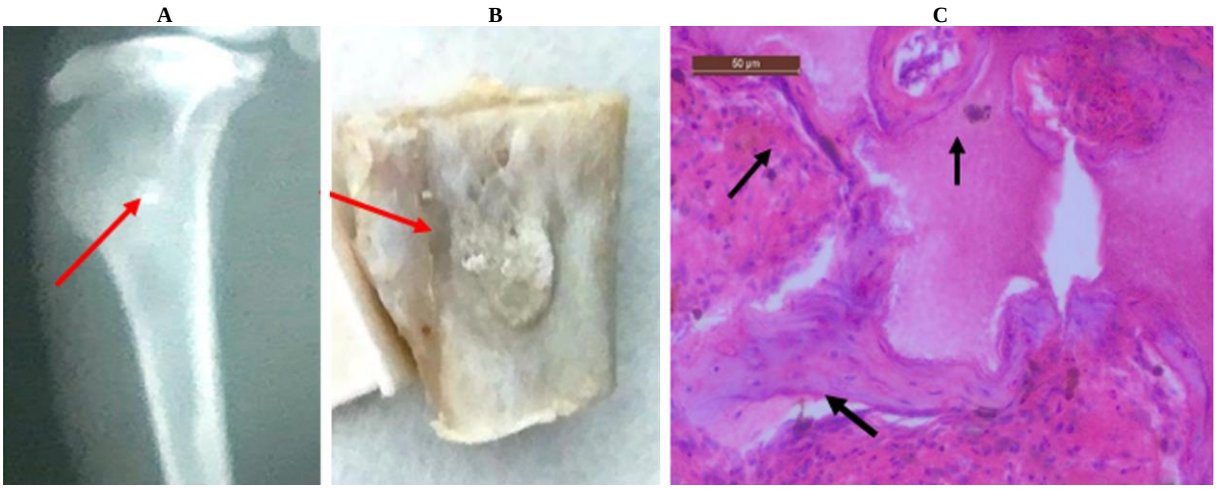



**Figure 9. Day 60. Characteristics of the integration processes of BIO implants (A – radiological; B – macroscopic; C – histological)**

In the third group, on the 60th day, the presence of an implanted composite was detected radiologically. Its X-ray density was similar to that on day 30. On macro-preparation, the implantation site did not visually differ from those in animals of other groups; it also had the appearance of periosteal bone growths (**Figure 7B**) and was covered with massive layers of hyaline cartilage. Histologically, the picture was similar to that in the 2nd group. The specimen demonstrated granules of fine-grained eosinophilic homogeneous mass with signs of minor fragmentation and destruction. Strips (beams) of course-fibrous bone tissue formed individual cells. The formation of lamellar bone tissue (secondary cancellous bone) was observed in the bone beams – the transitional stage from the third to the fourth stage of reparative bone regeneration (from immature reticulofibrous to mature lamellar bone tissue). This is the evidence of a faster course of regeneration, compared to the first and fourth groups on the 60th day (**Figure 10**).

In the fourth group, the implanted composite was visualized on radiographs as an area of increased radiodensity that completely filled the defect, as on the 30th day. On macro-preparation, the implantation site did not visually differ from those in animals of other groups of this period, and had the appearance of periosteal bone growths (covered with minor layers of hyaline cartilage, as in the second group. Histological examination revealed signs of minor fragmentation and destruction of the granules. Beams of course-fibrous bone tissue formed separate cells, which were filled with fibrous connective tissue – this is typical for the third stage of reparative regeneration with the formation of weakly mineralized reticulofibrous bone. Signs at the beginning of the transition to the fourth stage of reparative osteogenesis were noted directly on the surface of the granules (**Figure 11**).

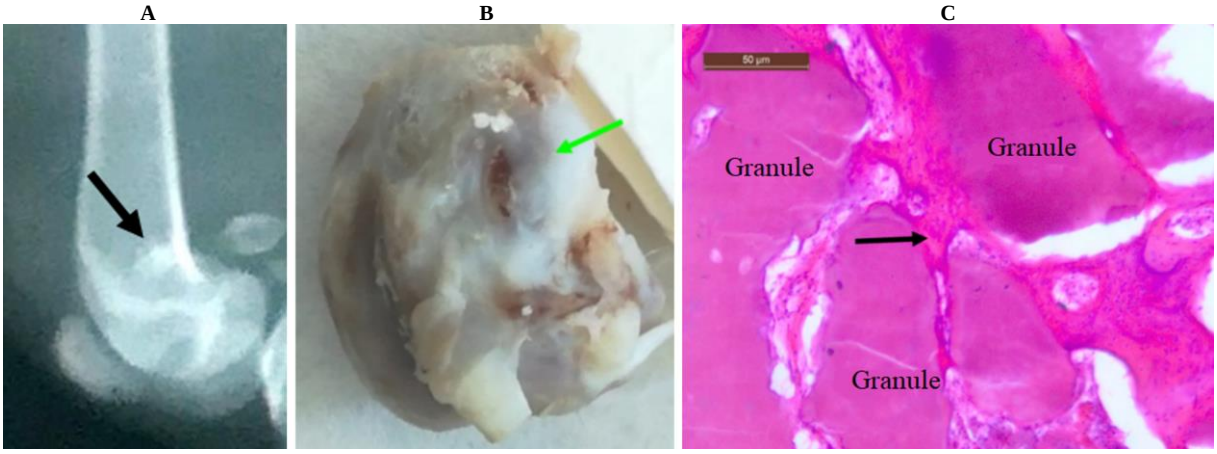



**Figure 10. Day 60. Characteristics of the integration processes of HTdSi+PRF implants (A – radiological; B – macroscopic; C – histological)**

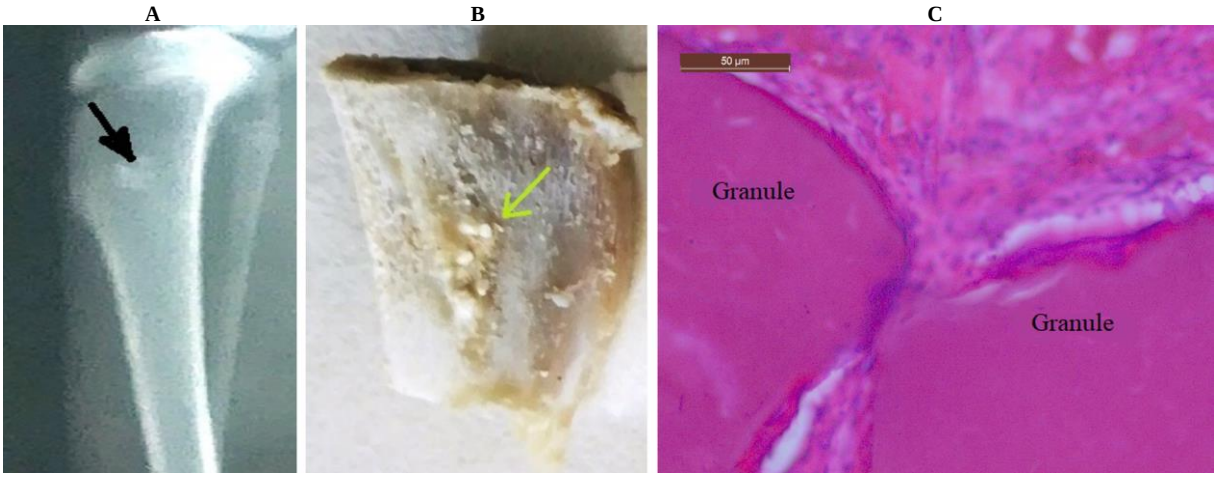



**Figure 11. Day 60. Characteristics of the integration processes of HTdSi implants (A – radiological; B – macroscopic; C – histological)**

On the 90th day, the traces of implants in the animals of the first group (BIO + PRF), were detected on X-ray images, which confirms the fact of resorption of this implant sample. On macro-preparation, the implantation site showed signs of remodeling of the newly formed periosteal bone – the regenerate mass decreased, and the cartilaginous layers were transformed into the bone tissue. Histologically, the regeneration was mainly represented by bone beams made of coarse fibrous bone tissue with a small amount of lamellar bone tissue in the middle. Here, the bone formation was at a transitional stage from the 3rd to the 4th stage of reparative regeneration with a predominance of reticulofibrous – immature bone tissue. The composite granules had the appearance of an areactive eosinophilic mass with signs of particle destruction in the form of round-oval conglomerates (**Figure 12**).

In the second group, as well as in the first one, the traces of biocomposite were found on the X-ray photographs, which indicates the fact of resorption of this ceramic sample. The implantation site on the macro-preparation site was almost not visualized, and signs of remodeling of newly formed periosteal bone and transformation of cartilaginous layers into bone tissue were noted. In the process of histological examination, the picture was as follows: the spongy substance in the form of beams of lamellar and coarse-fibrous bone tissue was in a ratio of 1:1. The ingrowth of the latter sample into the surface layers of the composite was also noted. This histopattern is typical for the transitional stage from the 3rd to the 4th stage of reparative regeneration with the same amount of reticulofibrous and lamellar bone tissue (**Figure 13**).

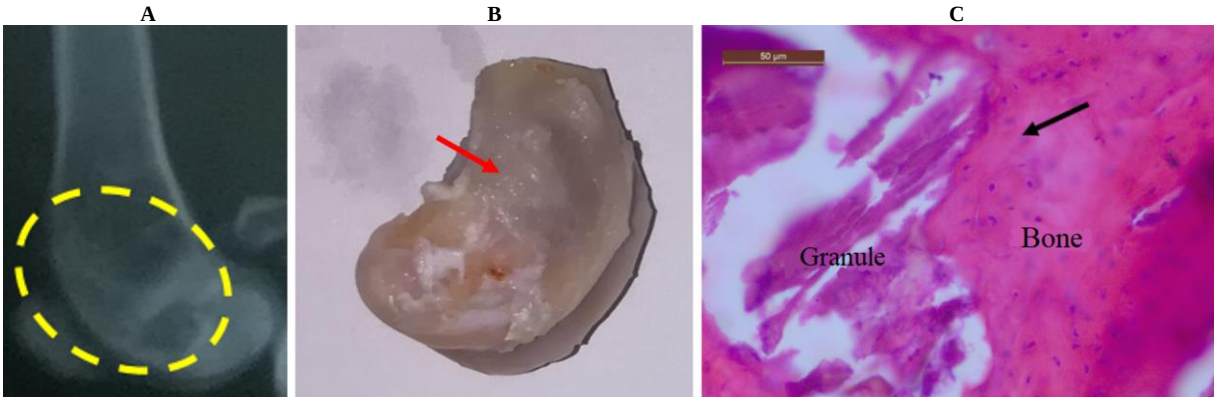



**Figure 12. Day 90. Characteristics of the integration processes of BIO+PRF implants (A – radiological; B – macroscopic; C – histological)**

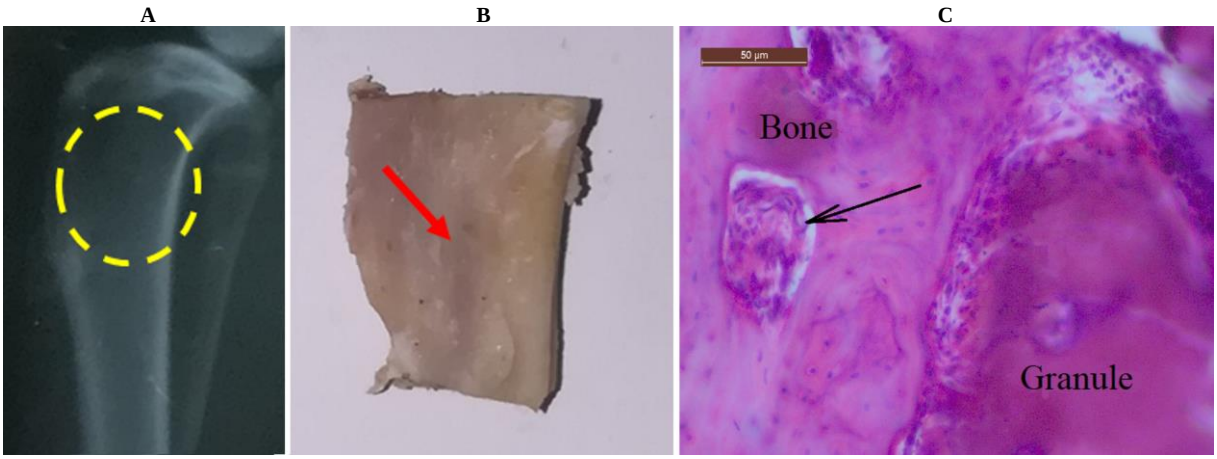



**Figure 13. Day 90. Characteristics of the integration processes of BIO implants (A – radiological; B – macroscopic; C – histological)**

At the same time, on the 90th day, the implant was well visualized on X-rays in rabbits of the 3rd group, which indicates its low resorptive properties. On the macro-preparation, the implantation site also showed signs of remodeling of the newly formed periosteal bone, and it was not particularly different from that in animals of other groups. Histologically, the consisted has been represented by beams, in which the lamellar bone tissue prevails (about 70%). The ingrowth of bone tissue occurred not only in the surface, but also in the middle layers of the composite. The transitional stage from the 3rd to the 4th stage of reparative regeneration with a predominance of lamellar bone tissue was more mature, compared to the rabbits of the first group (**Figure 14**).

The implanted composite was clearly visualized on X-rays in the animals of the 4th group, the signs of its resorption were not observed, as in the third group. On macro-preparation, the implantation site also showed signs of remodeling of the newly formed periosteal bone, the granules of the composite were enclosed in the newly formed bone tissue that filled the defect. Histologically, the spongy bone substance is represented by beams with a slight predominance of course-fibrous bone tissue. Newly formed bone tissue began to grow into the surface layers of the composite. The osteohistogenesis process of a spongy bone substance in the sites filled with hydroxyapatite ceramics HTdSi on the 90th day indicates a transitional stage from the 3rd to the 4th stage of reparative regeneration with a slight predominance of course-fibrous bone tissue (**Figure 15**).

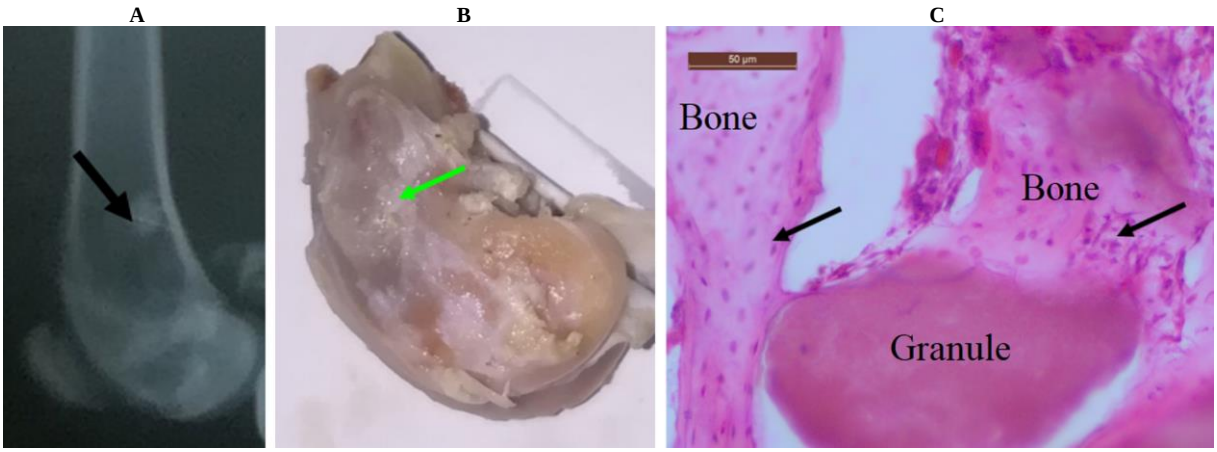



**Figure 14. Day 90. Characteristics of the integration processes of HTdSi+PRF implants (A – radiological; B – macroscopic; C – histological)**

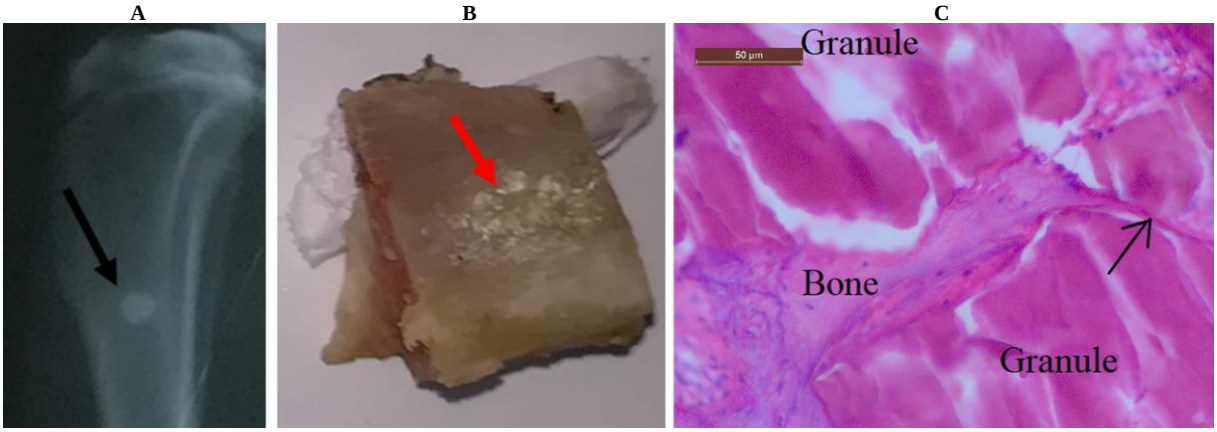



**Figure 15. Day 90. Characteristics of the integration processes of HTdSi implants (A – X-ray; B – macroscopic; C – histological)**

Six months later, traces of implants were not detected on radiographs in the animals of the first group (BIO + PRF). On macro-preparation, the implantation site had a typical formed bone tissue. Histologically, the spongy bone substance is represented by beams of course-fibrous and lamellar bone tissue in a ratio of 1:1. However, in the depth of bone structures, as it turned out, the regeneration processes were not yet fully completed, although they were at the final stages – the transitional stage from the 3rd to the 4$^{th}$ stage. Coarse-fibrous bone tissue grew into the surface layers of the composite (**Figure 16**).

In the second group, the implanted composite material was also not visualized on radiographs. A typical formed bone tissue was found on the macro-preparation at the implantation site. Histologically, in the spongy substance formed, lamellar bone predominated over beams of course-fibrous bone tissue. The processes of reparative regeneration were a feature of the incomplete fourth stage with insignificant residues of course-fiber bone tissue and its spread into the middle of the conglomerates (**Figure 17**).

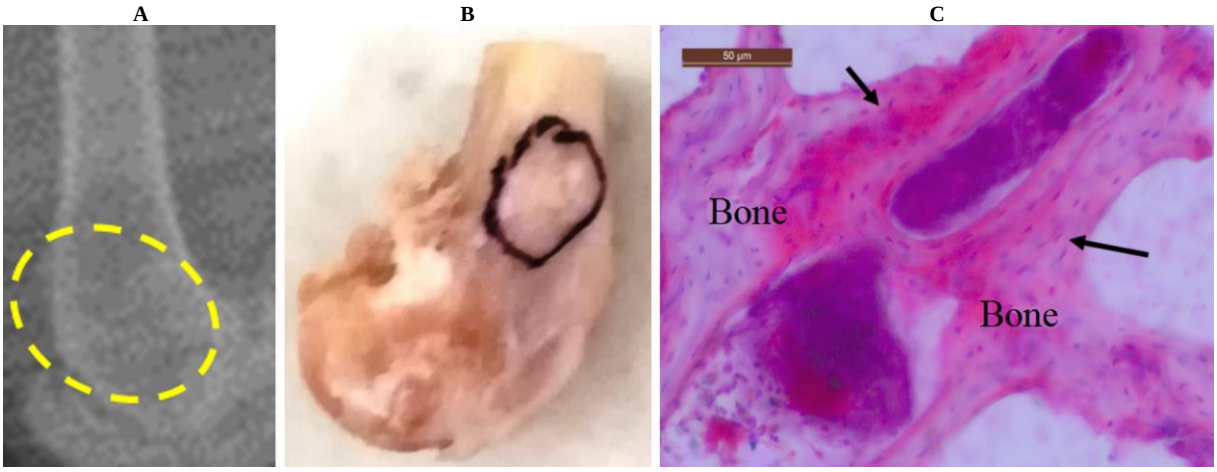



**Figure 16. Day 180. Characteristics of the integration processes of implants BIO + PRF (A – X-ray; B – macroscopic; C – histological)**

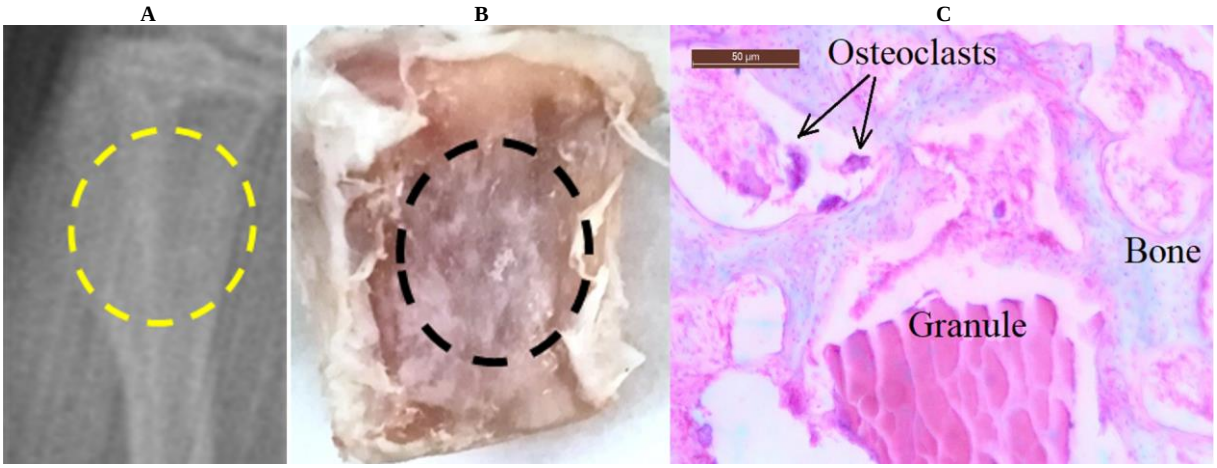



**Figure 17. Day 180. Characteristics of the integration processes of BIO implants (A – radiological; B – macroscopic; C – histological)**

At the same time, the traces of implants in the form of areas of increased X-ray density were found in the animals of 3rd group during this period, which indicates the slow resorption processes. On the macro-preparation, the implantation site also had a similar formed bone tissue with light interspersed granules that had the appearance of white islands embedded in the bone. Histologically, it has been found that reticulofibrous tissue is observed only in the middle of composite conglomerates, mainly in deep layers. The cancellous bone substance is built from beams of lamellar bone tissue, indicating a fully completed fourth stage of reparative bone regeneration (**Figure 18**).

In the animals of the 4th group, the traces of implants were detected on the X-rays in the form of areas of slightly increased radiodensity at this period, as well as in the 3rd group, which is a sign of a slow resorption process. On the macro-preparation, the implantation site also had similar formed bone tissue with interspersed granules in the form of white particles embedded in the bone tissue. Histologically, the ingrowth of course-fibrous bone tissue into the surface and middle layers of the composite was noted (**Figure 19**).

The spongy bone substance is represented by the beams of course-fibrous and lamellar bone tissue with a predominance of the latter one, and the processes of reparative regeneration were a feature of the transition from the 3rd to the 4th stage at the completion stage.

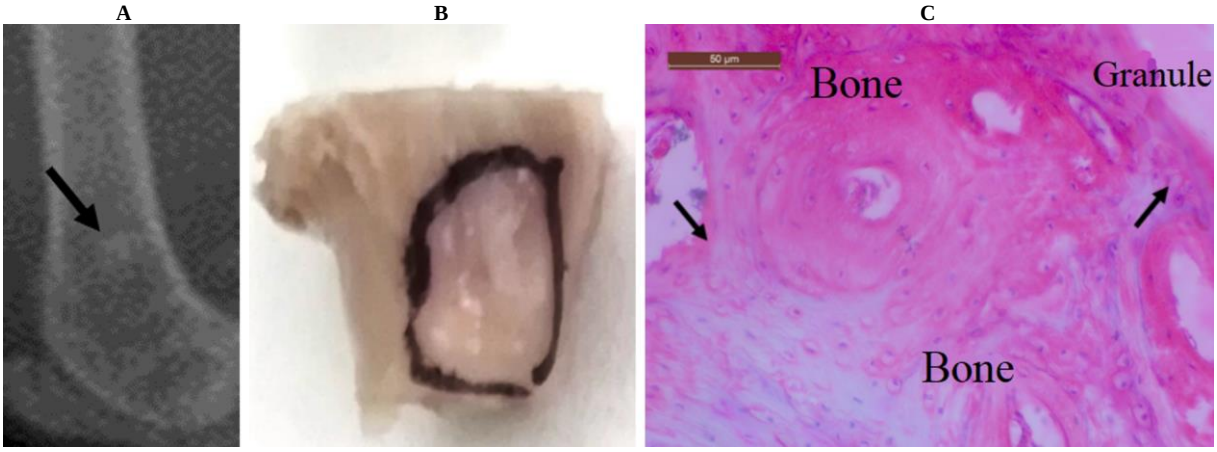



**Figure 18. Day 180. Characteristics of the integration processes of HTdSi + PRF implants (A – radiological; B – macroscopic; C – histological)**

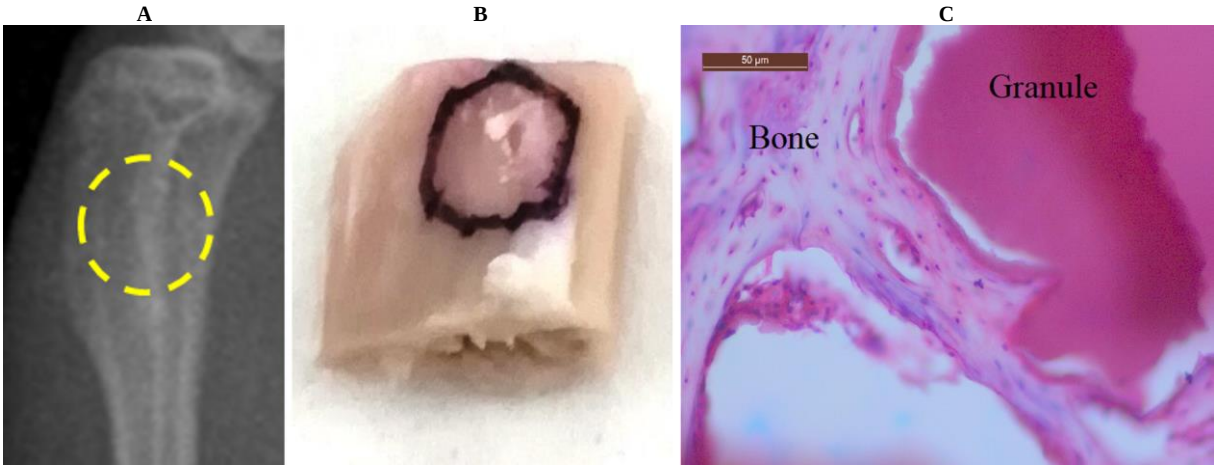



**Figure 19. Day 180. Characteristics of the integration processes of HTdSi implants (A – X-ray; B – macroscopic; C – histological)**

## Discussion

One of the most popular methods of increasing the CPC bioactivity is to increase its solubility by increasing the more soluble β-TCP phase in composition. That is why there is great interest in tricalcium phosphate, the solubility of which is much higher than that of HAP.[7,8,11,12] β-TCP is known to promote osteoblast formation, it is readily resorbed by macrophages and osteoclasts, and it is associated with a lower risk of failure or complications. However, the better solubility of β-TCP does not always lead to the expected result – replacing the implant with a full-fledged bone tissue, since its crystal structure differs from the crystal structure of the mineral component of bone tissue.[7,8,11,12,23] Preclinical studies and the results of the clinical use of β-TCP indicate that the rapid resorption of CPC often leads to the fact that full-fledged bone tissue does not have time to form in the defect volume, and that the β-TCP effect on osteogenesis is very limited.[23] In cases of plastic surgery of large bone defects, it is important that biomaterial is not only replaced by full-fledged bone tissue, but also maintains the strength of the defect area until the bone is completely restored. For this, it must have a resorption rate identical to the speed of new bone tissue formation, as well as osteoinductive properties for rapid integration of material with the regenerate throughout the entire defect volume and stimulation of its replacement with full-fledged bone tissue. The results of long-term experiments with β-TCP indicate that it can only possess osteoconductive properties.[16,24]

Numerous studies of bone tissue replacement with calcium-phosphate ceramics have shown the important role of porosity in this process.[19,24] Volumetric porosity and pore size affect the ability of CPC to promote vascularization, cell proliferation and osteoconduction *in vivo*.[24] It has been found that the pores of at least 40 μm are required for bone ingrowth, while the interconnected pores with diameters greater than 100 μm are required for implant integration. Characterization of the porous architecture of CPC is important for its effectiveness *in vivo*. At the beginning of histological studies of the replacement of bioactive ceramics with bone tissue, it has been concluded that only macropores with a size of 100-1000 microns are important for porous ceramics, while all other pores in size have only a negative effect due to a decrease in the strength of bioceramics. Further studies of the effect of pores on the replacement character of bioactive ceramics by bone tissue have shown that micropores are able to contribute to the increase of material resorption in a physiological environment. With the development of nanotechnology and the production of nanostructured bioactive ceramics, including the availability of nano-sized pores, it was determined that such ceramics have osteoinductive properties due to interaction with bone tissue at the cellular level. This gives the prospect of fully replacing autografts with bioactive ceramics.[20,25-28] Therefore, bioactive ceramics should have pores of different sizes, which should connect to each other as much as possible, while its strength should be sufficient to withstand the load on the defect until integration with bone tissue and penetration of the regenerate into the pore structure of the material.

In numerous publications, there is an unambiguous emphasis on the importance of the presence of nano-sized pores in CPC. It has been shown that a larger number of micropores enhance the adsorption of proteins such as fibrinogen.[19,20,24,27] The crystallinity and solubility of CPC also affect the cell adhesion by influencing the concentration of adsorbed proteins, as well as by influencing the pH and concentration of ions in an environment. For example, Q. Hu et al.[28] showed that the bone marrow stromal cells of rabbit adhere better to crystalline HAP, rather than to amorphous calcium phosphate of comparable size, although its solubility is significantly higher than that of HAP. S. Samavedi et al.[20] has also demonstrated that cranial vault osteoblasts of rats attach better to HAP surfaces with higher crystallinity than to HAP surfaces with lower crystallinity or to amorphous calcium phosphate. Research in the field of phosphate biomaterials in recent years has shown that anionic substitutions of phosphate ions for silicate ions can increase the bioactivity of CPC.[7,29-31] Silicon is an important element of connective and bone tissue. The elasticity and flexibility of tendons, articular cartilages and vessel walls depend on it. According to the literature data, silicon is a key element in biomineralization processes associated with the differentiation and reproduction of osteoblasts, their collagen synthesis, reconstruction, osteoclast development and resorption.[32,33]

Currently, ceramic materials based on HAP and silicon are of great interest. It was established that the presence of silicate in the HAP crystal lattice increases the material bioactivity, stimulates cellular activity, and promotes the matching of the implant with the bone, which is generally associated with the activation of osteoblasts and osteoclasts by silicon, which is released during the material dissolution. It is also believed that the increase in bioactivity can be a consequence of the physical and chemical modification of the replaced material, namely: changes in the chemical composition of the surface layer, morphology and microstructure.[34-38] The high activity of Si-CPC is associated with the formation of silanol -SiOH groups on the surface of the material, which together with ions of calcium and phosphate, create a synergistic effect concerning the impact on reparative processes in the bone tissue.[35,39-41] Studies have shown that hydroxylapatite modified with silicate-ions (Si-HAP) has an augmented surface electronegativity that contains hydrophilic Si-OH groups that easily interact with polar groups of organic compounds, facilitating cell attachment and promoting the formation of a larger number of the implant-bone connections. Si-HAP was studied for solubility both *in vitro* and *in vivo*, in comparison with pure HAP, where it was shown that silicon in the structure of HAP increases the solubility of the material regardless of the method of studying the HAP solubility.[42-45]

Another way to increase the bioactive properties of CPC is to use it in combination with platelet-rich fibrin. Platelet-rich fibrin, which is a second-generation platelet concentrate, is actively used in the treatment of intraosseous defects to stimulate bone regeneration in situ as an independent defect filler and in combination with allografts and β-TCP.[46-51] PRF is an environment of autologous fibrin, in which a large number of platelets and leukocyte cytokines are embedded during centrifugation. The internal integration of cytokines into the fibrin mesh ensures their gradual release within 7-10 days as the fibrin mesh disintegrates. According to A. Simonpieri et al.[52] data, fibrin supports and protects the transplanted biomaterial, and PRF fragments serve as biological connectors between bone particles (mechanical role). The integration of this chain of fibrin clots into the regenerative area facilitates the cell migration, especially of endothelial cells, which are essential for neoangiogenesis, vascularization and graft survival.[53,54] Platelet growth factors (platelet growth factor, beta-transforming growth factor, insulin-like growth factor-1) are gradually released during resorption of the fibrin matrix, which leads to the phenomenon of long-term healing. Leukocytes and cytokines present in the fibrin matrix can contribute to the self-regulation of inflammatory and infectious phenomena in the transplanted material. Thus, the properties of this natural biomaterial, namely fibrin, open up a great potential for wound healing.[55-61]

## Conclusions

Replacement of the bone defects with granules of BIO and HTdSi ceramics in the form of monocomponents showed certain differences. In particular, at all stages of research, the regeneration of bone tissue was faster in the animals of the second group (BIO sample), rather than in the fourth group (HTdSi sample). In the later periods (90th and 180th day), the histological examination showed almost the same results. However, the combination of the BIO sample with PRF led to a delay in reparative processes in this group at the initial stages. The filling of defects with granules of domestic HTdSi ceramics in combination with PRF showed that the regeneration of bone tissue with their participation begins at earlier stages and proceeds faster, compared to the BIO sample. This is possible due to the properties provided by silicon in the ceramic structure, the presence of a nanostructure, and the presence of a less soluble HAP phase in HTdSi. It is the rapid dissolution of BIO that causes some inhibition of the regeneration processes in connection with the load of the cells of osteoclast programmed differentiation, which ensure the resorption of the implant as a foreign object. At the same time, the HTdSi biomaterial with gradual resorption did not cause an excessive reaction of osteoblasts and it was included in the regeneration processes at the early stages, which accelerated the healing of defects.

The combination of HTdSi with PRF made it possible to accelerate regeneration processes already at the early stages, as confirmed by the histological picture in the first and third groups. This was also evidenced by the appearance of a large number of layers of hyaline cartilage on the newly formed periosteal bone of the defect zone in the respective groups, which was noted on the 30th and 60th day, and which was later transformed into the bone tissue. Therefore, according to the study results of the osseointegration properties of ceramics both as independent components and in combination with PRF, the groups can be arranged in the following sequence BIO + PRF<HTdSi<BIO<HTdSi + PRF.

## References

1. Xin H, Xu L, Yuli S, Feng Q, Gang C. Current Trends in Research on Bone Regeneration: A Bibliometric Analysis. Biomed Res Int. 2020: 8787394. https://doi.org/10.1155/2020/8787394
2. El-Ghannam AR. Advanced bioceramic composite for bone tissue engineering: design principles and structure-bioactivity relationship. J Biomed Mater Res A. 2004;69(3):490-501. https://doi.org/10.1002/jbm.a.30022
3. Guoke T, Zhiqin L, Jiangming Yu, Xing W, Zhihong T, Xiaojian Y. 2021. Recent Trends in the Development of Bone Regenerative Biomaterials. Front Cell Dev Biol. 2021;9:665813. https://doi.org/10.3389/fcell.2021.665813
4. Navarro M, Michiardi A, Castano O, Planell J. Biomaterials in orthopaedics. J R Soc Interface. 2008;5(27):1137-1158. https://doi.org/10.1098/rsif.2008.0151
5. Gloivacki J, Mulliken JB. Demineralized bone implants. Clin Plast Surg. 1985;12(2):233-241. https://doi.org/10.1016/S0094-1298(20)31694-1
6. Buck BE, Malinin TI, Brown MD. 1989. Bone transplantation and human immunodeficiency virus. An estimate of risk of aquired immunodeficiency syndrome. Clin Orthop Relat Res. 1989;(240):129-136.
7. Ziman ZZ. Calcium phosphate biomaterials. KhNU named after VN Karazin; 2018.
8. Barinov SM, Komlev VS. Bioceramics based on calcium phosphates. Nauka; 2005.
9. Slutsky L, Vetra Y. Biological issues of biomaterials science. Latvian Medical Academy; 2001.

10. Dorozhkin SV. Biphasic, triphasic and multiphasic calcium orthophosphates. Acta Biomater. 2012;8(3):963-977. https://doi.org/10.1016/j.actbio.2011.09.003
11. Dorozhkin SV. Calcium orthophosphate-based bioceramics. Materials (Basel). 2013;6(9):3840-3942. https://doi.org/10.3390/ma6093840
12. LeGeros RZ. Biodegradation and bioresorption of calcium phosphate ceramics. Clin Mater. 1993;14(1):65-88. https://doi.org/10.1016/0267-6605(93)90049-d
13. LeGeros RZ. Properties of osteoconductive biomaterials: calcium phosphates. Clin Orthop Relat Res. 2002;(395):81-98. https://doi.org/10.1097/00003086-200202000-00009
14. Nathanael JA, Oyane A, Nakamura M, Koga K, Nishida E, Tanaka S, Miyaji H. Calcium phosphate coating on dental composite resins by a laser-assisted biomimetic process. Heliyon. 2018;4(8):e00734. https://doi.org/10.1016/j.heliyon.2018.e00734
15. Pepla E, Besharat LK, Palaia G, Tenore G, Migliau G. Nano-hydroxyapatite and its applications in preventive, restorative and regenerative dentistry: a review of literature. Ann Stomatol (Roma). 2014 20;5(3):108-114.
16. El-Ghannam A. Bone reconstruction: from bioceramics to tissue engineering. Expert Rev Med Devices. 2005;2(1):87-101. https://doi.org/10.1586/17434440.2.1.87
17. Narayan RJ. The next generation of biomaterial development. Philos Trans R Soc A Math Phys Eng Sci. 2010;368(1917):1831-1837. https://doi.org/10.1098/rsta.2010.0001
18. Uvarova IV, Gorbik PP, Gorobets SV, Ivashchenko OA, Ulyanchich NV. Nanomaterials for medical purposes. Naukova Dumka; 2014.
19. Gauthier O, Bouler JM, Aguado E, Pilet P, Daculsi G. Macroporous biphasic calcium phosphate ceramics: influence of macropore diameter and macroporosity percentage on bone ingrowth. Biomaterials. 1998;19(1-3):133-139. https://doi.org/10.1016/s0142-9612(97)00180-4
20. Samavedi S, Whittington AR, Goldstein AS. Calcium phosphate ceramics in bone tissue engineering: A review of properties and their influence on cell behavior. Acta Biomater. 2013;9(9):8037-8045. https://doi.org/10.1016/j.actbio.2013.06.014
21. Muñoz‐Corcuera M, Bascones‐Martínez A, Ripollés RJ. Post‐extraction application of beta tricalcium phosphate in alveolar socket. J Osseointegration. 2015;7(1):8‐14. https://doi.org/10.23805/jo.2015.07.01.02
22. Habibovica P, Yuanb H, Van Der Valkb CM, Meijerc G, Van Blitterswijka CA, De Groot K. 3D microenvironment as essential element for osteoinduction by biomaterials. Biomaterials. 2005;26(17):3565-3575. https://doi.org/10.1016/j.biomaterials.2004.09.056
23. Liu B, Lun DX. 2012. Current application of β-tricalcium phosphate composites in orthopaedics. Orthop Surg. 2012;4(3):139-144. https://doi.org/10.1111/j.1757-7861.2012.00189.x
24. Ezzahmouly M, Elmoutaouakkil A, Ed-Dhahraouy M, Khallok H, Elouahli A, Mazurier A, ElAlbani A, Hatim Z. Micro-computed tomographic and SEM study of porous bioceramics using an adaptive method based on the mathematical morphological operations. Heliyon. 2019;5(12):e02557. https://doi.org/10.1016/j.heliyon.2019.e02557.
25. Truite CVR, Noronha JNG, Prado GC, Santos LN, Palácios RS, Do Nascimento A, et al. Bioperformance Studies of Biphasic Calcium Phosphate Scaffolds Extracted from Fish Bones Impregnated with Free Curcumin and Complexed with Cyclodextrin in Bone Regeneration. Biomolecules. 2022;12(3):383. https://doi.org/10.3390/biom12030383
26. Eliaz N, Metoki N. Calcium Phosphate Bioceramics: A Review of Their History, Structure, Properties, Coating Technologies and Biomedical. Materials (Basel). 2017;10(4):334. https://doi.org/10.3390/ma10040334
27. Ebrahimi M. Biomimetic principle for development of nanocomposite biomaterials in tissue engineering. In: Inamuddin AM, Asiri AM, ed. Applications of Nanocomposite Materials in Orthopedics. Woodhead; 2018:287-306.
28. Hu Q, Tan Z, Liu Y, Tao J, Cai Y, Zhang M, Pan H, Xu X, Tang R. Effect of crystallinity of calcium phosphate nanoparticles on adhesion, proliferation, and differentiation of bone marrow mesenchymal stem cells. J. Mater. Chem. 2007;17:4690-4698. https://doi.org/10.1039/B710936A
29. Dorozhkin SV, Epple M. Biological and medical significance of calcium phosphates. Angew Chem Int Ed Engl. 2002;41(17):3130-3146. https://doi.org/10.1002/1521-3773(20020902)41:17<3130::AID-ANIE3130>3.0.CO;2-1
30. Astala R, Calderin I, Yin X, Stott MJ. Ab initio simulation of Si-doped hydroxyapatite. Chem Mater. 2005;18(2):413-422. https://doi.org/10.1021/cm051989x
31. Rau JV, Cacciotti I, Laureti S, Fosra M, Varvaro G, Latini A. Bioactive, nanostructured Si-substituted hydroxyapatite coatings on titanium prepared by pulsed laser deposition. J Biomed Mater Res B Appl Biomater. 2015;103(8):1621-1631. https://doi.org/10.1002/jbm.b.33344
32. Hing KA, Revell PA, Smith N, Buckland T. Effect of silicon level on rate, quality and progression of bone healing within silicatesubstituted porous hydroxyapatite scaffolds. Biomaterials. 2006;27(29):5014-5026. https://doi.org/10.1016/j.biomaterials.2006.05.039
33. Szurkowska K, Szeleszczuk L, Kolmas J. Effects of Synthesis Conditions on the Formation of Si-Substituted Alpha Tricalcium Phosphates. Int J Mol Sci. 2020;21(23):9164. https://doi.org/10.3390/ijms21239164

34. Carlisle EM. Silicon: a possible factor in bone calcification. Science. 1970;167(3916):279-280. https://doi.org/10.1126/science.167.3916.279
35. Tavafoghi M, Kinsella JM, Gamys CG, Gosselin M, Zhao YF. Silicon-doped hydroxyapatite prepared by a thermal technique for hard tissue engineering applications. Ceram Int. 2018;44(15):17612-17622. https://doi.org/10.1016/j.ceramint.2018.06.071
36. Kudłacik-Kramarczyk S, Drabczyk A, Głąb M, Dulian P, et al. Mechanochemical synthesis and investigations of calcium titanate powders and their acrylic dispersions. J Eur Ceram Soc. 2014;34(10):2259-2264. https://doi.org/10.3390/ma13153275
37. Sahalevych AI, Sergiychuk RV, Ozhohin VV, Khrapchuk AYu, Dubovyi YO, Frolov OS. The Modified Procedure of Totally Tubeless PNL. Int J Biol Biomed Engin. 2022;16:82-89. https://doi.org/10.46300/91011.2022.16.10
38. Sobczak-Kupiec A, Olender E, Malina D, Tyliszczak B. Effect of calcination parameters on behavior of bone hydroxyapatite in artificial saliva and its biosafety. Mater Chem Phys. 2018;206:158-165. https://doi.org/10.1016/j.matchemphys.2017.12.020
39. Porter AE, Botelho CM, Lopes MA, Santos JD, Best SM, Bonfield W. Ultrastructural comparison of dissolution and apatite precipitation on hydroxyapatite and silicon-substituted hydroxyapatite in vitro and in vivo. J Biomed Mater Res A. 2004;69(4):670-679. https://doi.org/10.1002/jbm.a.30035
40. Sahalevych A, Sergiychuk R, Ozhohin V, Vozianov O, Khrapchuk A, Dubovyi Y, Frolov O. Mini-percutaneous nephrolithotomy in surgery of Nephrolithiasis. Ukrain J Nephrol Dialys. 2021;(3):44-52.
41. Sobczak-Kupiec A, Malina D, Tyliszczak B, Piatkowski M, Bialik-Was K, Wzorek Z. Evaluation of bioactivity of Poly(Acrylic acid) - hydroxyapatite - nanogold composites in in vitro conditions. Digest J Nanomat Biostruct. 2012;7(2):459-467.
42. Tang Q, Brooks R, Rushton N, Best S. Production and characterization of HA and SiHA coatings. J Mater Sci Mater Med. 2010;21(1):173-181. https://doi.org/10.1007/s10856-009-3841-y
43. Tyliszczak B, Pielichowski K. Novel hydrogels containing nanosilver for biomedical applications - Synthesis and characterization. J Polym Res. 2013;20(7):191. https://doi.org/10.1007/s10965-013-0191-8
44. Polatova DSh, Islamov UF, Davletov RR, Savkin AV, Sharipov MM. Oncologic outcomes of pelvic bone sarcomas surgical. Int J Health Sci. 2021;5(3):252-259. https://doi.org/10.53730/ijhs.v5n3.1467
45. Navruzov SN, Polatova DSh, Gafoor-Akhunov MA, Gabdikarimov KH. The value of marker proteins p53, bcl-2, Ki-67 in predicting the effectiveness of treatment for osteogenic sarcoma of tubular bones. Vopr Onkol. 2012;58(5):691-693.
46. Das S, Jhingran R, Bains VK, Madan R, Srivastava R, Rizvi I. Socket preservation by beta-tri-calcium phosphate with collagen compared to platelet-rich fibrin: A clinico-radiographic study. Eur J Dent. 2016;10(2):264-276. https://doi.org/10.4103/1305-7456.178298.
47. Sakibaev KS, Nikityuk DB, Alekseyeva NT, Klochkova SV, Tashmatova NM. Characteristics of muscle mass in women of different constitutions. Res J Pharm Technol. 2019;12(12):6193-7.
48. Takahashi Y, Marukawa E, Omura K. 2013. Application of a new material (ß‑TCP/collagen composites) in extraction socket preservation. Int J Oral Maxillofac Implants. 2013;28(2):444-452. https://doi.org/10.11607/jomi.2794
49. Gadipelly S, Sultana S, Venkatesh VV, Praveen P. Comparative Radiological Analysis of Efficacy of Beta-tricalcium Phosphate and Beta-tricalciumPhosphate with Platelet-rich Fibrin in MaxillarySinus Augmentation – A Clinical Study. Indian J Dent Adv. 2019; 10(4):171-175. https://doi.org/10.5866/2018.10.10171
50. Elmohandes W. Evaluation of beta tricalcium phosphate mixed with platelet rich fibrin for rehabilitation of atrophic maxilla with implant installation. J Oral Maxillofac. Surg. 2013;42(10):1261. https://doi.org/10.1016/j.ijom.2013.07.303
51. Alan H, Kavak G, Nergiz Y, Tunik S, Yavuz I. Comparative Investigation of The Effects of Platelet-Rich Plasma in Sinus Lifting. IAMR. 2015;7(2):1-12.
52. Simonpieri A, Del Corso M, Sammartino G, Dohan Ehrenfest DM. The relevance of Choukroun's platelet‑rich fibrin and metronidazole during complex maxillary rehabilitations using bone allograft. Part I: a new grafting protocol. Implant Dent. 2009;18(2):102-111. https://doi.org/10.1097/ID.0b013e318198cf00
53. Dmytriiev D, Dmytriiev K, Stoliarchuk O, Semenenko A. Multiple organ dysfunction syndrome: What do we know about pain management? A narrative review. Anaesth Pain Intensive Care. 2019;23(1):84-91.
54. Serniak YP, Sagalevych AI, Frolov OS, Serniak PY, Kryvopustov MS. Extraperitoneoscopic radical prostatectomy after pelvic sugery procedures. Wiad Lek. 2020;73(6):1093-1096.
55. Peleg M, Garg AK, Mazor Z. Predictability of simultaneous implant placement in the severely atrophic posterior maxilla. Int J Oral Maxillofac Implants. 2006;21(1):94-102.
56. Barhate UH, Mangaraj M, Jena AK, Sharan J. Applications of Platelet Rich Fibrin in Dental Surgery. Trends Biomater Artif Organs. 2021;35(2):203-213.
57. Simon BI, Zatcoff AL, Kong JJ, O'Connell SM. Clinical and histological comparison of extraction socket healing following the use of autologous platelet‑rich fibrin matrix (PRFM) to ridge preservation procedures emploting demineralized freeze-dried bone allograft material and membrane. Open Dent J. 2009;3:92-99. https://doi.org/10.2174/1874210600903010092

58. Choukroun J, Diss A, Simonpieri A, Girard MO, Schoeffler C, Dohan SL, Dohan AJJ, Mouhyi J, Dohan DM. Platelet‐rich fibrin (PRF): A second‐generation platelet concentrate: Histologic evaluations of PRF effects on bone allograft maturation in sinus lift. Oral Surg Oral Med Oral Pathol Oral Radiol Endod. 2006;101(3):299-303. https://doi.org/10.1016/j.tripleo.2005.07.012

59. Gupta SJ, Jhingran R, Gupta V, Bains VK, Madan R, Rizvi I. Efficacy of platelet‐rich fibrin vs. enamel matrix derivative in the treatment of periodontal intrabony defects. J Int Acad Periodontol. 2014;16(3):86-96.

60. Mathur A, Bains VK, Gupta V, Jhingran R, Singh GP. Evaluation of intrabony defects treated with platelet‐rich fibrin or autogenous bone graft. Eur J Dent. 2015;9(1):100-108. https://doi.org/10.4103/1305-7456.149653

61. Gupta V, Bains VK, Singh GP, Mathur A, Bains R. Regenerative potential of platelet rich fibrin in dentistry: literature review. AJOHAS. 2011;1(1):22‐28.